Müller Formulation for Analysis of Scattering from 3-D Dielectric Objects with Triangular Patching Model

Chang-Hyun Lee*, Jin-Sang Cho, Baek-Ho Jung† and Tapan K. Sarkar*****

Abstract – In this paper, we present a set of numerical schemes to solve the Müller integral equation for the analysis of electromagnetic scattering from arbitrarily shaped three-dimensional (3-D) dielectric bodies by applying the method of moments (MoM). The piecewise homogeneous dielectric structure is approximated by planar triangular patches. A set of the RWG (Rao, Wilton, Glisson) functions is used for expansion of the equivalent electric and magnetic current densities and a combination of the RWG function and its orthogonal component is used for testing. The objective of this paper is to illustrate that only some testing procedures for the Müller integral equation yield a valid solution even at a frequency corresponding to an internal resonance of the structure. Numerical results for a dielectric sphere are presented and compared with solutions obtained using other formulations.

Keywords: Dielectric, Electromagnetic scattering, Method of moments, Müller integral equation

1. Introduction

In the analysis of dielectric bodies at frequencies that correspond to an internal resonance of the structure, spurious solutions are obtained for the electric field integral equation (EFIE) or the magnetic field integral equation (MFIE). One possible way of obtaining a unique solution at an internal resonant frequency of the structure under analysis is to combine a weighted linear sum of the EFIE with MFIE and thereby eliminate the spurious solutions. This combination results in the combined field integral equation (CFIE). One may also obtain the PMCHW (Poggio, Miller, Chang, Harrington, Wu) and Müller integral equations [1], [2]. Many publications are available for the analysis of a dielectric body using the CFIE. However, most of the earlier techniques have been utilized to solve two-dimensional problems and bodies of revolution.

To analyze 3-D objects using a surface integral equation, triangular patch modeling can be used. The triangular patches have the ability to conform to any geometrical surface or boundary, permitting easy descriptions of the patching scheme to the computer. A suitable basis function for the triangle patch is the RWG function presented in [3]. Sheng *et al.* proposed the CFIE for the analysis of scattering from arbitrarily shaped 3-D dielectric bodies [4]. In their work, the electric and magnetic currents are expanded using the RWG functions, and a combination of RWG and its orthogonal component, which is point-wise spatially orthogonal to the original set, is used for testing. Jung *et al.* also investigated a set of CFIE formulations by choosing a combination of testing functions and dropping one of the testing terms in the CFIE [5]. Although several integral equation formulations have been used for 3-D dielectric bodies [4-8], the Müller integral equation has not been applied for the analysis of scattering by arbitrarily shaped 3-D dielectric objects with triangular patch modeling.

In this paper, we present a numerical scheme to solve the Müller integral equation for the analysis of electromagnetic scattering from arbitrarily shaped three-dimensional (3-D) piecewise homogeneous dielectric objects. For this, the equivalent currents are expanded using the RWG functions, and a combination of the RWG function and its orthogonal component is used for testing. We investigate all possible cases of the testing procedure using the four parameters in conjunction with the testing functions. In the next section, we describe the integral equation formulations and testing procedures. Section 3 presents numerical results and compares them. Finally, conclusions are presented in section 4.

2. Integral Equations

In this section, we discuss the integral equations for a

† Corresponding Auther: Department of Information and Communication Engineering, Hoseo University, Asan, Chungnam 336-795, Korea. (bhjung@hoseo.edu)
* Ethertronics, SK Ventium Bldg 522, Dangjeong-dong, Gunpo, Gyeonggi 435-776, Korea. (elecjour@kiee.or.kr)
** Department of Information and Communication Engineering, Graduate School, Hoseo University, Asan, Chungnam 336-795, Korea. (j_s_cho@naver.com)
*** Department of Electrical Engineering and Computer Science, Syracuse University, Syracuse, NY 13244-1240, USA. (tksarkar@syr.edu)
Received 21 July 2006 ; Accepted 4 February, 2007

dielectric scatterer, which is illuminated by an electromagnetic wave [5]. We consider a homogeneous dielectric body with a permittivity ε_2 and a permeability μ_2 placed in an infinite homogeneous medium with a permittivity ε_1 and a permeability μ_1, as shown in Fig. 1.

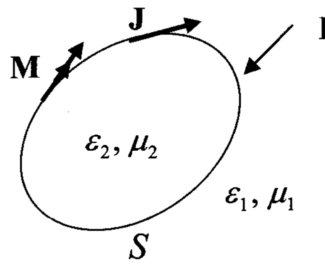

Fig. 1 Homogeneous dielectric body illuminated by an electromagnetic wave.

By invoking the equivalence principle, the integral equation is formulated in terms of the equivalent electric and magnetic current densities $\mathbf{J}$ and $\mathbf{M}$ on the surface S of the dielectric body. By enforcing the continuity of the tangential electric and magnetic fields at S, the following integral equations are obtained:

$$\left[-\mathbf{E}_1^s(\mathbf{J},\mathbf{M})\right]_{\tan} = \left[\mathbf{E}^i\right]_{\tan} \tag{1}$$

$$\left[-\mathbf{E}_2^s(\mathbf{J},\mathbf{M})\right]_{\tan} = 0 \tag{2}$$

$$\left[-\mathbf{H}_1^s(\mathbf{J},\mathbf{M})\right]_{\tan} = \left[\mathbf{H}^i\right]_{\tan} \tag{3}$$

$$\left[-\mathbf{H}_2^s(\mathbf{J},\mathbf{M})\right]_{\tan} = 0 \tag{4}$$

where $\mathbf{E}^i$ and $\mathbf{H}^i$ are the incident electric and magnetic fields, respectively. The subscript 'tan' denotes the tangential component. The scattered electric and magnetic fields, $\mathbf{E}_\nu^s$ and $\mathbf{H}_\nu^s$, are given by

$$\mathbf{E}_\nu^s(\mathbf{J}) = -j\omega\mathbf{A}_\nu - \nabla\Phi_\nu \tag{5}$$

$$\mathbf{E}_\nu^s(\mathbf{M}) = -\frac{1}{\varepsilon_\nu}\nabla\times\mathbf{F}_\nu \tag{6}$$

$$\mathbf{H}_\nu^s(\mathbf{M}) = -j\omega\mathbf{F}_\nu - \nabla\Psi_\nu \tag{7}$$

$$\mathbf{H}_\nu^s(\mathbf{J}) = \frac{1}{\varepsilon_\nu}\nabla\times\mathbf{A}_\nu \tag{8}$$

where ν is 1 or 2. In Equations (5) to (8), $\mathbf{A}_\nu$ and $\mathbf{F}_\nu$ are the magnetic and electric vector potentials, and Φ_ν and Ψ_ν are the electric and magnetic scalar potentials, respectively.

In (1)-(4), there are two unknowns $\mathbf{J}$ and $\mathbf{M}$, and four equations relating them. It is possible to develop various combinations for the solution of these equations [1], [2]. If we take only two equations, (1) and (2), we have the EFIE formulation. Dual to the EFIE formulation, we can obtain the MFIE formulation by choosing only (3) and (4). However, both EFIE and MFIE formulations fail at frequencies at which the surface S, when covered by a perfect electric conductor and filled with the materials of the exterior medium, forms a resonant cavity. For the CFIE formulation, a set of two integral equations are formed from the set (1)-(4) using the following form

$$(1-\kappa)\left[-\mathbf{E}_\nu^s(\mathbf{J},\mathbf{M})\right]_{\tan} + \kappa\eta_\nu\left[-\mathbf{H}_\nu^s(\mathbf{J},\mathbf{M})\right]_{\tan} = \begin{cases}(1-\kappa)\left[\mathbf{E}^i\right]_{\tan} + \kappa\eta_1\left[\mathbf{H}^i\right]_{\tan}, \nu = 1 \\ 0, \nu = 2\end{cases} \tag{9}$$

where κ is the usual combination parameter, which can have any value between 0 and 1, and η_ν is the wave impedance of region ν. As an alternative way of combining the four equations, the set of four equations is reduced to two by adding (1) to (2) and (3) to (4). This gives a pair of equations

$$\left[-\mathbf{E}_1^s(\mathbf{J},\mathbf{M}) - \alpha\mathbf{E}_2^s(\mathbf{J},\mathbf{M})\right]_{\tan} = \left[\mathbf{E}^i\right]_{\tan} \tag{10}$$

$$\left[-\mathbf{H}_1^s(\mathbf{J},\mathbf{M}) - \beta\mathbf{H}_2^s(\mathbf{J},\mathbf{M})\right]_{\tan} = \left[\mathbf{H}^i\right]_{\tan} \tag{11}$$

where $\alpha = \varepsilon_1/\varepsilon_2$ and $\beta = \mu_1/\mu_2$. This is termed as the Müller formulation [2]. If $\alpha = \beta = 1$, then Eqs. (10) and (11) become the PMCHW formulation.

The surface of the dielectric structure to be analyzed is approximated by planar triangular patches. As in [3], we use the RWG function, $\mathbf{f}_n$, associated with the n-*th* common edge as the basis function. In general, the electric current density $\mathbf{J}$ and the magnetic current density $\mathbf{M}$ on the dielectric structure may be approximated in terms of this basis function as

$$\mathbf{J}(\mathbf{r}) = \sum_{n=1}^{N} J_n\mathbf{f}_n(\mathbf{r}) \tag{12}$$

$$\mathbf{M}(\mathbf{r}) = \sum_{n=1}^{N} M_n\mathbf{f}_n(\mathbf{r}) \tag{13}$$

where J_n and M_n are constants yet to be determined and N is the number of edges on the surface for the triangulated model approximating the surface of the dielectric body. In this work all of the equivalent currents, $\mathbf{J}$ and $\mathbf{M}$, are expanded as in (12) and (13). The next step in the numerical implementation scheme is to develop a testing procedure to transform the operator equation into a matrix equation using the MoM. In the CFIE formulation, (9), we may use a combination of RWG and its orthogonal component as the testing function to convert the integral equation into a matrix equation. The orthogonal function associated with the n-*th* common edge is defined through $\mathbf{g}_n = \mathbf{n}\times\mathbf{f}_n$. Here $\mathbf{n}$ is the normal unit pointing outward from the surface. The various numerical implementation schemes to solve the CFIE have been investigated in [4] and [5].

Now we consider the testing procedure for the Müller equation. By substituting (1)-(8) into (10) and (11) and extracting the Cauchy principal value from the curl term, we may rewrite (10) and (11) as, respectively,

$$\left[j\omega(\mathbf{A}_1+\alpha\mathbf{A}_2)+\nabla(\Phi_1+\alpha\Phi_2)+(1-\alpha)\frac{1}{2}\mathbf{n}\times\mathbf{M} + PV\left(\frac{1}{\varepsilon_1}\nabla\times\mathbf{F}_1+\alpha\frac{1}{\varepsilon_2}\nabla\times\mathbf{F}_2\right)\right]_{\tan} = \left[\mathbf{E}^i\right]_{\tan} \tag{14}$$

$$\left[j\omega(\mathbf{F}_1+\beta\mathbf{F}_2)+\nabla(\Psi_1+\beta\Psi_2)-(1-\beta)\frac{1}{2}\mathbf{n}\times\mathbf{J} - PV\left(\frac{1}{\mu_1}\nabla\times\mathbf{A}_1+\beta\frac{1}{\mu_2}\nabla\times\mathbf{A}_2\right)\right]_{\tan} = \left[\mathbf{H}^i\right]_{\tan} \tag{15}$$

where PV denotes the principal value. In the PMCHW formulation, $\alpha=\beta=1$. Therefore, from (14) and (15) we obtain

$$\sum_{\nu=1}^{2}\left[j\omega\mathbf{A}_\nu+\nabla\Phi_\nu+PV\left(\frac{1}{\varepsilon_\nu}\nabla\times\mathbf{F}_\nu\right)\right]_{\tan} = \left[\mathbf{E}^i\right]_{\tan} \tag{16}$$

$$\sum_{\nu=1}^{2}\left[j\omega\mathbf{F}_\nu+\nabla\Psi_\nu+PV\left(\frac{1}{\mu_\nu}\nabla\times\mathbf{A}_\nu\right)\right]_{\tan} = \left[\mathbf{H}^i\right]_{\tan} \tag{17}$$

In this PMCHW integral equation, the RWG function is used as the testing functions [4-6], yielding an accurate and stable solution. However, we need the spatially orthogonal component $\mathbf{g}_m$ in addition to the RWG function for the Müller equation in order to test the third term $\mathbf{n}\times\mathbf{M}$ and $\mathbf{n}\times\mathbf{J}$ in (14) and (15) as well. Now, we present a general expression for testing Müller equations using the following

Table 1 Testing method for various integral equations and the average difference of bistatic RCS between Mie series and numerical solutions for the dielectric sphere.

Formulation		Testing method		ΔRCS (dBm^2)	Example
CFIE		$<\mathbf{f}_m+\mathbf{g}_m,\ \mathbf{E}>$	$<-\mathbf{f}_m+\mathbf{g}_m,\ \mathbf{H}>$	0.44	Fig. 3
PMCHW		$<\mathbf{f}_m,\ \mathbf{E}>$	$<\mathbf{f}_m,\ \mathbf{H}>$	0.19	
Müller	TETH	$<\mathbf{f}_m,\ \mathbf{E}>$	$<\mathbf{f}_m,\ \mathbf{H}>$	0.24	
	NENH	$<\mathbf{g}_m,\ \mathbf{E}>$	$<\mathbf{g}_m,\ \mathbf{H}>$	2.10	
	TENE -THNH	$<\mathbf{f}_m+\mathbf{g}_m,\ \mathbf{E}>$	$<\mathbf{f}_m+\mathbf{g}_m,\ \mathbf{H}>$	*0.12*	Fig. 4(a)
			$<\mathbf{f}_m-\mathbf{g}_m,\ \mathbf{H}>$	*0.14*	
		$<\mathbf{f}_m-\mathbf{g}_m,\ \mathbf{E}>$	$<\mathbf{f}_m+\mathbf{g}_m,\ \mathbf{H}>$	*0.10*	Fig. 4(b)
			$<\mathbf{f}_m-\mathbf{g}_m,\ \mathbf{H}>$	*0.16*	
	TENE-TH	$<\mathbf{f}_m+\mathbf{g}_m,\ \mathbf{E}>$	$<\mathbf{f}_m,\ \mathbf{H}>$	0.31	Fig. 5(a)
		$<\mathbf{f}_m-\mathbf{g}_m,\ \mathbf{E}>$		0.34	
	TENE-NH	$<\mathbf{f}_m+\mathbf{g}_m,\ \mathbf{E}>$	$<\mathbf{g}_m,\ \mathbf{H}>$	2.38	Fig. 5(b)
		$<\mathbf{f}_m-\mathbf{g}_m,\ \mathbf{E}>$		2.15	
	TE-THNH	$<\mathbf{f}_m,\ \mathbf{E}>$	$<\mathbf{f}_m+\mathbf{g}_m,\ \mathbf{H}>$	0.14	Fig. 6(a)
			$<\mathbf{f}_m-\mathbf{g}_m,\ \mathbf{H}>$	0.19	
	NE-THNH	$<\mathbf{g}_m,\ \mathbf{E}>$	$<\mathbf{f}_m+\mathbf{g}_m,\ \mathbf{H}>$	1.62	Fig. 6(b)
			$<\mathbf{f}_m-\mathbf{g}_m,\ \mathbf{H}>$	2.07	

four parameters in conjunction with the testing functions as

$$\begin{aligned}&\left\langle f_E\mathbf{f}_m + g_E\mathbf{g}_m, -\mathbf{E}_1^s(\mathbf{J},\mathbf{M}) - \alpha\mathbf{E}_2^s(\mathbf{J},\mathbf{M})\right\rangle \\ &= \left\langle f_E\mathbf{f}_m + g_E\mathbf{g}_m, \mathbf{E}^i\right\rangle\end{aligned} \tag{18}$$

$$\begin{aligned}&\left\langle f_H\mathbf{f}_m + g_H\mathbf{g}_m, -\mathbf{H}_1^s(\mathbf{J},\mathbf{M}) - \beta\mathbf{H}_2^s(\mathbf{J},\mathbf{M})\right\rangle \\ &= \left\langle f_H\mathbf{f}_m + g_H\mathbf{g}_m, \mathbf{H}^i\right\rangle\end{aligned} \tag{19}$$

where the testing coefficients, f_E, g_E, f_H, and g_H, may be +1 or -1. This equation may be termed as the TENE-THNH formulation as in [5]. By choosing different testing coefficients, we have four different cases for the Müller formulation. They are summarized along with the appropriate testing coefficients in Table 1. It was also suggested to drop one of the testing terms in the CFIE formulation [4, 5]. Applying this scheme to (18) and (19), we obtain four formulations named as TENE-TH ($g_H = 0$), TENE-NH ($f_H = 0$), TE-THNH ($g_E = 0$), and NE-THNH ($f_E = 0$), depending on which term is neglected. By a selecting a different sign for the testing coefficients, one may have eight possible cases of testing with different testing coefficients, which are summarized in Table 1. In the CFIE formulation, one may choose $\mathbf{f}_m + \mathbf{g}_m$ for the electric field part and $-\mathbf{f}_m + \mathbf{g}_m$ for the magnetic field part as the testing function [5]. Note it is possible to choose the testing functions as $\mathbf{f}_m - \mathbf{g}_m$ for the electric field part and $\mathbf{f}_m + \mathbf{g}_m$ for the magnetic field part as in [5].

3. Numerical Examples

In this section, we present and compare the numerical results obtained from several integral equation formulations discussed in the above section. To illustrate the methodology, we consider a dielectric sphere having a diameter of 1 m and a relative permittivity ε_r=4, centered at the origin, as shown in Fig. 2. The surface of the sphere is modeled with 1,224 triangular patches, which resulted in a total of 1,836 edges. In the numerical calculation, the sphere is illuminated from the top by an incident x-polarized plane wave with the propagation vector $\hat{\mathbf{k}} = -\hat{\mathbf{z}}$. The numerical results to be shown are the bistatic radar cross section (RCS) solutions of the sphere at 262 MHz, which is the first resonant frequency of the sphere. Table 1 also shows the average difference between the numerical and Mie solutions for the bistatic RCS of the sphere at the $\phi = 0^\circ$ plane. The averaged difference of the bistatic RCS is computed by using the definition

$$\Delta RCS = \frac{\sum_1^M \left|\text{RCS(Mie)} - \text{RCS(Numerical)}\right|}{M} \tag{20}$$

where M is the number of samples. In all the legends of figures to be shown, the four numbers in the parentheses mean the testing coefficients, (f_E, g_E, f_H, g_H), introduced in (18) and (19).

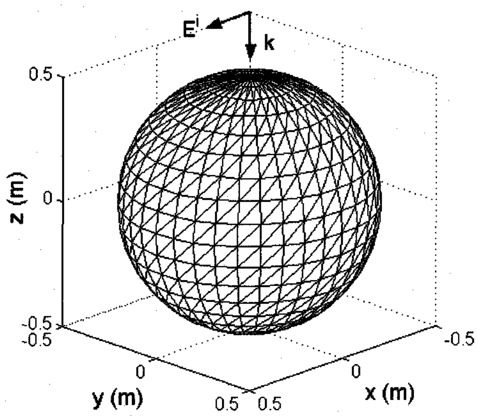

Fig. 2 Triangular surface patching of a dielectric sphere with ε_r=4, 0.5 m of a radius. 1,224 patches and 1,836 edges.

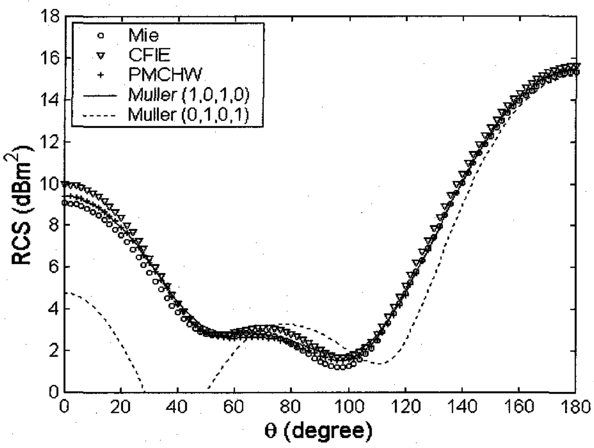

Fig. 3 Bistatic RCS of the dielectric sphere computed by CFIE, PMCHW, and Müller (TETH and NENH) formulations.

As a first example, Fig. 3 shows the bistatic RCS solutions obtained from CFIE, PMCHW and Müller (TETH and NENH) formulations, and compares those with the Mie series solution. The CFIE solution is computed using the testing coefficients as f_E=1, g_E=1, f_H=-1, and g_H=1 with the combination parameter of $\kappa = 0.5$ in (9). If we look carefully at Fig. 3, we observe there is an agreement between the Müller (TETH) and PMCHW solutions. The reason for this is that the RWG function does not test the term $\mathbf{n}\times\mathbf{M}$ and $\mathbf{n}\times\mathbf{J}$ in (14) and (15) well, resulting in a solution similar to the PMCHW. All of the numerical results except the NENH do not exhibit the spurious resonance and agree well with the Mie solution.

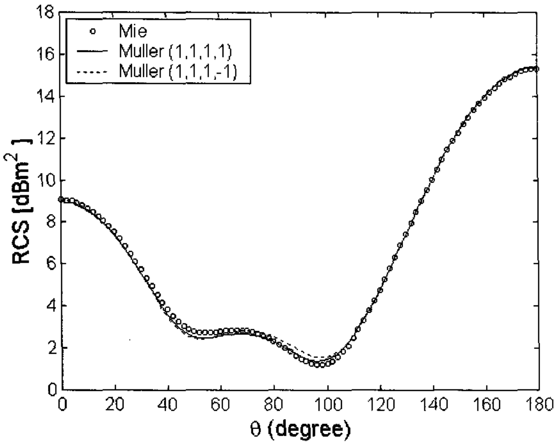

(a)

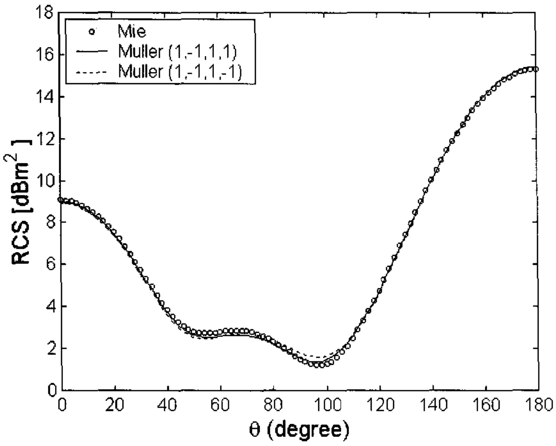

(b)

Fig. 4 Bistatic RCS of the dielectric sphere computed by Müller formulations (TENE-THNH). (a) $<\mathbf{f}_m+\mathbf{g}_m,\ \mathbf{E}>$ and $<\mathbf{f}_m\pm\mathbf{g}_m,\ \mathbf{H}>$, (b) $<\mathbf{f}_m-\mathbf{g}_m,\ \mathbf{E}>$ and $<\mathbf{f}_m\pm\mathbf{g}_m,\ \mathbf{H}>$.

As a second example, Fig. 4 shows the bistatic RCS solutions computed from the four cases of TENE-THNH formulation, and compares them with the Mie solution. All of the numerical results using the Müller equation do not exhibit the spurious resonance and agree well with the Mie solution. It is difficult to distinguish between the solutions. We also observe that the average difference for the four cases is smaller than that of the PMCHW and CFIE formulations as presented in Table 1. However, solutions for the equivalent currents using the two cases,

(i) $<\mathbf{f}_m-\mathbf{g}_m,\ \mathbf{E}>$ and $<\mathbf{f}_m+\mathbf{g}_m,\ \mathbf{H}>$

(ii) $<\mathbf{f}_m+\mathbf{g}_m,\ \mathbf{E}>$ and $<\mathbf{f}_m-\mathbf{g}_m,\ \mathbf{H}>$

are unstable in the low frequency region (0-100 MHz), not shown here.

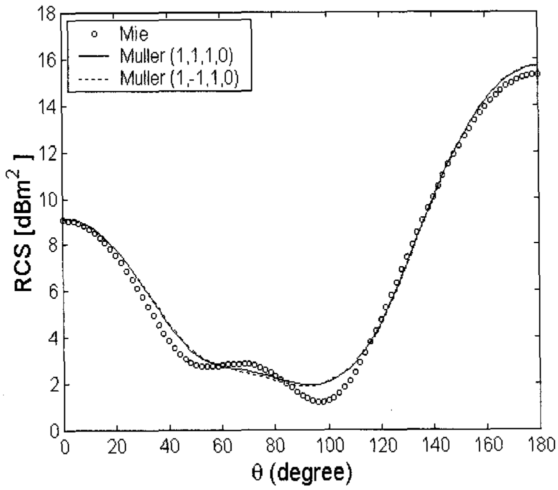

(a)

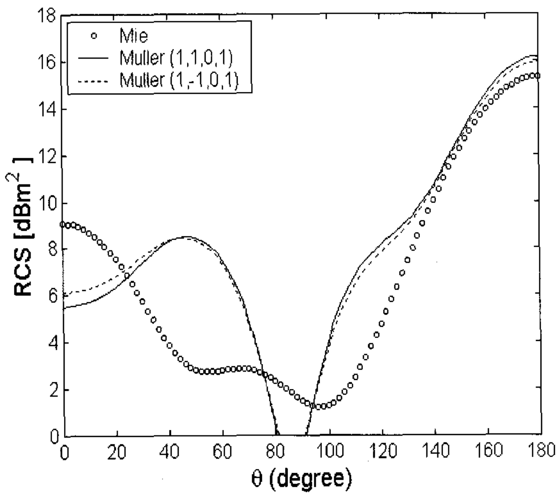

(b)

Fig. 5 Bistatic RCS of the dielectric sphere computed by Müller formulations. (a) TENE-TH, $<\mathbf{f}_m\pm\mathbf{g}_m,\ \mathbf{E}>$ and $<\mathbf{f}_m,\ \mathbf{H}>$, (b) TENE-NH, $<\mathbf{f}_m\pm\mathbf{g}_m,\ \mathbf{E}>$ and $<\mathbf{g}_m,\ \mathbf{H}>$.

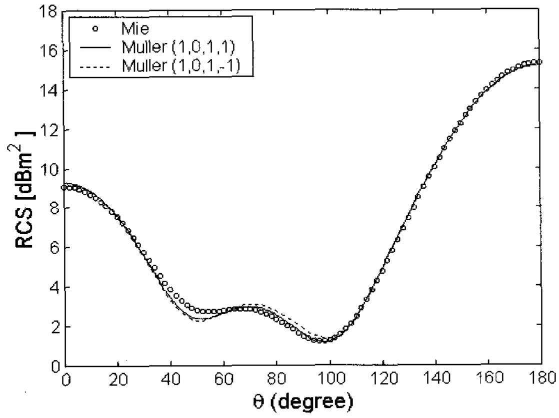

(a)

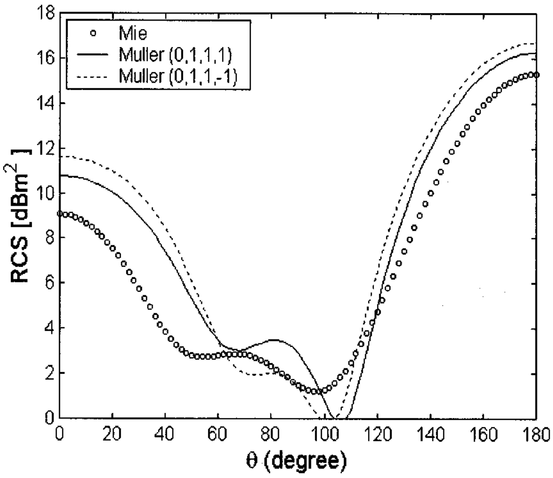

(b)

Fig. 6 Bistatic RCS of the dielectric sphere computed by Müller formulations. (a) TE-THNH, $<\mathbf{f}_m,\ \mathbf{E}>$ and $<\mathbf{f}_m \pm \mathbf{g}_m,\ \mathbf{H}>$, (b) NE-THNH, $<\mathbf{g}_m,\ \mathbf{E}>$ and $<\mathbf{f}_m \pm \mathbf{g}_m,\ \mathbf{H}>$.

Lastly, Figs. 5 and 6 show the bistatic RCS solutions using the scheme that drops one of the testing terms (8 cases). In Figs. 5(a) and 6(a), we observe that the TENE-TH and TE-THNH solutions agree with the Mie solution, but they are less accurate than the TENE-THNH solutions of Fig. 4. The average differences between the bistatic RCS are given in Table 1. It is interesting to note in Figs. 5(b) and 6(b) that the TENE-NH and NE-THNH solutions are inaccurate when testing (10) or (11) with $\mathbf{g}_m$ only.

4. Conclusion

The numerical scheme for solving the Müller integral equation is investigated to analyze scattering from 3-D arbitrarily shaped dielectric objects with the triangular patch model. To obtain a numerical solution, we employ the MoM in conjunction with the RWG basis function. The Müller formulation gives accurate and valid solutions at an internal resonant frequency of the scatterer, only when testing both of the electric and magnetic fields with the combination of the RWG function and its orthogonal component at the same time. All the solutions obtained by using TENE-TH and TE-THNH formulations dropping one of the testing terms are less accurate. The NE-THNH and TENE-NH formulations, testing one of the Müller equations with $\mathbf{g}_m$ only, do not give valid solutions. Finally, we propose two testing methods for the Müller equation that are not affected by the internal resonance problem and yield a stable solution even at low frequency by choosing either RWG $+\mathbf{n}\times$ RWG or RWG $-\mathbf{n}\times$ RWG for testing the electric and magnetic fields simultaneously.

Acknowledgements

This work was supported by an Academic Research Fund of Hoseo University under Grant 20040330.

References

[1] J. R. Mautz and R. F. Harrington, "Electromagnetic scattering from a homogeneous material body of revolution," *Arch. Elektron. Ubertragungstech.*, vol. 33, pp. 71-80, 1979.

[2] R. F. Harrington, "Boundary integral formulations for homogeneous material bodies," *J. Electromagn. Waves Applicat.*, vol. 3, no. 1, pp. 1-15, 1989.

[3] S. M. Rao, D. R. Wilton, and A. W. Glisson, "Electromagnetic scattering by surfaces of arbitrary shape," *IEEE Trans. Antennas Propagat.*, vol. 30, no. 5, pp. 409-418, May 1982.

[4] X. Q. Sheng, J. M. Jin, J. M. Song, W. C. Chew, and C. C. Lu, "Solution of combined-field integral equation using multilevel fast multipole algorithm for scattering by homogeneous bodies," *IEEE Trans. Antennas Propagat.*, vol. 46, no. 11, pp. 1718-1726, Nov. 1998.

[5] B. H. Jung, T. K. Sarkar, and Y.-S. Chung, "A survey of various frequency domain integral equations for the analysis of scattering from three-dimensional dielectric objects," *J. of Electromagn. Waves and Applicat.*, vol. 16. no. 10, pp. 1419-1421, 2002.

[6] K. Umashankar, A. Taflove, and S. M. Rao, "Electromagnetic scattering by arbitrary shaped three-dimensional homogeneous lossy dielectric bodies," *IEEE Trans. Antennas Propagat.*, vol. 34, no. 6, pp. 758-766, June 1986.

[7] S. M. Rao and D. R. Wilton, "*E*-field, *H*-field, and combined field solution for arbitrarily shaped three-dimensional dielectric bodies," *Electromagn.*, vol. 10, pp. 407-421, 1990.

[8] S. Yeung, "Single integral equation for electromagnetic scattering by three-dimensional homogeneous dielectric objects," *IEEE Trans. Antennas Propagat.*, vol. 47, no. 10, pp. 1615-1622, Oct. 1999.

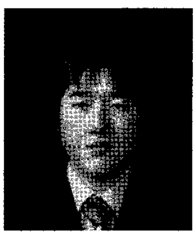

Chang-Hyun Lee
He received B.S. and M.S. degrees in Information and Communication Engineering from Hoseo University, Korea, in 2005 and 2007, respectively. He is currently an engineer in Ethertronics, Korea. His research interests are in antenna design and technology.

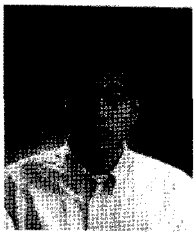

Jin-Sang Cho
He received B.S. degree in Information and Communication Engineering from Hoseo University, Korea, in 2006 and is working towards his M.S. degree in Information and Communication Engineering. His research interests are in time and frequency domain computational electromagnetics.

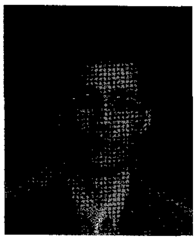

Baek-Ho Jung
He received the B.S., M.S., and Ph.D. degrees in electronic and electrical engineering from Kyungpook National University, Taegu, Korea, in 1986, 1989, and 1997, respectively. From 1989 to 1994, he was a Researcher with the Agency for Defense Development in Korea. Since 1997, he has been a Lecturer and is currently an Associate Professor with the Department of Information and Communication Engineering, Hoseo University, Asan, Chungnam, Korea, He was a Visiting Scholar with Syracuse University, Syracuse, NY, from 2001 to 2003. His current research interests are computational electromagnetics and wave propagation.

Tapan K. Sarkar
He received the B.Tech. degree from the Indian Institute of Technology, Kharagpur, in 1969, the M.Sc.E. degree from the University of New Brunswick, Fredericton, NB, Canada, in 1971, and the M.S. and Ph.D. degrees from Syracuse University, Syracuse, NY, in 1975. From 1975 to 1976, he was with the TACO Division of the General Instruments Corporation. He was with the Rochester Institute of Technology, Rochester, NY, from 1976 to 1985. He was a Research Fellow at the Gordon McKay Laboratory, Harvard University, Cambridge, MA, from 1977 to 1978. He is now a Professor in the Department of Electrical and Computer Engineering, Syracuse University and concurrently president of OHRN Enterprises, a small business established in 1985 in New York State to implement various theories to the solution of various challenging electromagnetic and signal processing problems. His current research interests deal with numerical solutions of operator equations arising in electromagnetics and signal processing with application to system design. He has authored or coauthored more than 280 journal articles and numerous conference papers and 32 chapters in books and 15 books, including his most recent ones, *History of Wireless* (John Wiley & Sons, 2005), *Smart Antennas* (John Wiley & Sons, 2003), *Wavelet Applications in Electromagnetics and Signal Processing* (Boston, MA, Artech House, 2002), and *Iterative and Self-Adaptive Finite-Elements in Electromagnetic Modeling* (Boston, MA, Artech House, 1998). He is a Registered Professional Engineer in the State of New York. Dr. Sarkar received a "Best Solution" award in May 1977 from the Rome Air Development Center (RADC) Spectral Estimation Workshop. He received the Best Paper Award of the IEEE Transactions on Electromagnetic Compatibility in 1979 and in the 1997 National Radar Conference. He received the College of Engineering Research Award in 1996 and the Chancellor's Citation for Excellence in Research in 1998 at Syracuse University. He was an Associate Editor for feature articles of the *IEEE Antennas and Propagation Society Newsletter* (1986-1988). He was the Chairman of the Inter-commission Working Group of International URSI on Time Domain Metrology (1990–1996). He was a distinguished lecturer for the Antennas and Propagation Society from 2000 to 2003. He is currently a member of the IEEE Electromagnetics Award Board and an Associate Editor for the IEEE Transactions on Antennas and Propagation. He is the Vice president of the Applied Computational Electromagnetics Society (ACES) and the Technical Chair for the combined IEEE 2005 Wireless Conference along with ACES to be held in Hawaii. He is on the editorial board of the *Journal of Electromagnetic Waves and Applications* and *Microwave and Optical Technology Letters*. He is a member of Sigma Xi and International Union of Radio Science Commissions A and B. He received Docteur Honoris Causa both from Universite Blaise Pascal, Clermont Ferrand, France, in 1998 and from the Politechnic University of Madrid, Madrid, Spain, in 2004. He received the medal of the *friend of the city of Clermont Ferrand*, in 2000.